Enhanced Metal-Insulator Transition Performance in Scalable Vanadium Dioxide Thin Films Prepared Using a Moisture-Assisted Chemical Solution Approach

Weizheng Liang, [†] Min Gao, [*,†] Chang Lu, [†] Zhi Zhang, [‡] Cheuk Ho Chan, [‡] Lanjian Zhuge, [§] Jiyan Dai, [‡] Hao Yang, [‖] Chonglin Chen, [⊥] Bae Ho Park, [#] Quanxi Jia, [#,◊] and Yuan Lin [*,†]

[†] State Key Laboratory of Electronic Thin films and Integrated Devices, University of Electronic Science and Technology of China, Chengdu, Sichuan 610054, P. R. China.

[‡] Department of Applied Physics, The Hong Kong Polytechnic University, Hong Kong, P.R. China.

[§] Analysis and Testing Center, Soochow University, Suzhou, 215123, P.R. China.

[‖] College of Science, Nanjing University of Aeronautics and Astronautics, Nanjing, 211106, P.R. China.

[⊥] Department of Physics and Astronomy, University of Texas at San Antonio, San Antonio, Texas 78249, USA.

[#] Division of Quantum Phases & Devices, Department of Physics, Konkuk University, Seoul, 143-701, Korea

1

◊Department of Materials Design and Innovation, University at Buffalo – The State of University of New York, Buffalo, New York 14260, USA.

ABSTRACT: Vanadium dioxide (VO_2) is a strong-correlated metal-oxide with a sharp metal-insulator transition (MIT) for broad device development. However, synthesizing epitaxial VO_2 films with desired properties has been a challenge due to the difficulty in controlling the oxygen stoichiometry of VO_x, where x can be in the range of $1 < x < 2.5$ and V has multiple valence states. Herein, a unique moisture-assisted chemical solution approach has been developed to successfully manipulate the oxygen stoichiometry, to significantly broaden the growth window, and to significantly enhance the MIT performance of VO_2 films. The obvious broadening of the growth window of stoichiometric VO_2 thin films, from 4°C to 36°C, is ascribed to a self-adjusted process for oxygen partial pressure at different temperatures by introducing moisture. A resistance change as large as four orders of magnitude has been achieved in VO_2 thin films with a sharp transition width of less than 1°C. The much enhanced MIT properties can be attributed to the higher and more uniform oxygen stoichiometry. It is not only scientific interesting but also technological important that this unique scalable technique for fabricating wafer-scaled VO_2 films with uniform properties has been successfully developed for practical device applications.

1. INTRODUCTION

Vanadium dioxide (VO_2), a classical strong-correlated oxide with a sharp metal-insulator transition (MIT), has fascinated scientists and engineers' insterests owing to its enrich chemical and physical properties for various novel device applications. During the MIT, the resistivity of VO_2 can change about 4-5 orders of magnitude, and its optical properties are also largely modulated.[1-3] These unique properties make VO_2 attractive for infrared detectors, smart windows, optical modulators, and thermal/electrical/optical-driving-switches used in microelectronic or optical-electronic devices. [1-6] However, the desired electrical and optical properties of VO_2 can only be achieved with the well-controlled oxygen stoichiometry.[2, 3] In other words, the nonstoichiometric VO_2 (either oxygen vacancy or non-desired V valence states) would break the correlation of V-V 3d electrons to alter electronic energy states and/or introduce strain in the films which result in the trends to unfavorable electronic and optical properties for device development. Since V has multi-valence states, the value of x in VO_x can be in the broad range of $1 \leq x \leq 2.5$,[5, 7] making the oxygen stoichiometry of VO_2 extremely susceptible to the growth condition. Thus, precisely controlling the oxygen stoichiometry in VO_x and establishing the role of oxygen stoichiometry for manipulating the metal-insulator transition have become the critical issues in the research community. [2, 3, 8, 9] It is well known that once the stoichiometry of VO_2 is deviated from its ideal value, the vanadium oxide Magnéli phases (V_nO_{2n-1}) with lower oxidation states (<+4) or the Wadsley phases (V_nO_{2n+1}) with higher oxidation states (>+4) can form (as seen in Figure S1). This implies that a robust processing technique with the ability to prevent the formation of V^{5+} or V^{3+} during the growth process becomes necessary for governing high performance VO_2 films. Therefore, various techniques have been explored to fabricate highly stoichiometric VO_2 thin films.[3, 10, 11]

Thermodynamically, both the oxygen partial pressure pO_2 and the growth temperature can be used to control the valence states of V for stable phases of V_2O_3, VO_2 and V_2O_5, as seen in Figure 1 (a).[12] In the physical vapor deposition such as sputtering, pulsed laser deposition (PLD), and molecular beam epitaxy (MBE),[10, 13] the most common approach is to adjust the oxygen partial pressure pO_2 in the growth chamber under a growth temperature (denoted as strategy (a), or the arrow (a) shown in Figure 1 (a)).[13, 14] In the chemical solution deposition (CSD) techniques, the approach is usually to adjust the processing temperature under a constant oxygen pressure (denoted as strategy (b), or the arrow (b) shown in Figure 1 (a)).

Fan et al.[10] have grown VO_2 thin films using MBE with approach (a) and found that a large resistivity-drop across MIT was achieved with oxygen flow rates of 1.3 - 1.8 sccm during the film growth. Kim et al [14] deposited the films by changing the oxygen pressure using PLD and also found that highly stoichiometric VO_2 samples was achieved only with oxygen pressures varying from 30 to 50 mTorr. Meanwhile, Lee et al [13] showed that the oxygen pressure window during the process to grow highly stoichiometric VO_2 was very narrow (only 10 mTorr). In this paper, we have tried to obtain highly stoichiometric VO_2 thin films using the polymer-assisted deposition (PAD) technique by adopting strategy (b) to optimize the growth condition. PAD is a CSD technique whose distinguish feature is that inorganic metal ions are bonded with a water-soluble polymer to form the water-based precursor solution. Since the metal ions are bonded with the polymer, the hydrolytic reactions in water are avoided by the ligands that block the access of water molecules to the metal ions, which has greatly improved the stability and controllability of the process. Similar to other typical CSD techniques for thin film deposition, the precursor solution is applied onto a substrate and the coated layer is finally treated at a desired temperature in a proper environment to remove the polymer while the remained metal ions react with gas to form films.

By using this technique, the optimized growth temperature window for high quality VO_2 thin films with a resistance-drop across MIT larger than 2×10^3 times was found to be as narrow as 4°C, which will be shown in the following section. The very narrow growth window of high quality VO_2 is attributed to the multi-valence states of V ions and the complex phase diagram of VO_x. Therefore, it is still imperative to explore a practical way to control the oxygen stoichiometry and further improve the MIT properties of VO_2 thin films with scalable dimension and reproducible properties for practical applications.

Although the transition width of less than 1°C has been reported on a few high quality VO_2 thin films grown by MBE or PLD, [4, 15, 16] very limited efforts have been explored for enhancing MIT properties of VO_2 thin films grown by a CSD technique which offers great advantages of low cost and easy setup. Herein, we have systematically investigated the effects of oxygen content on the MIT properties of VO_2 thin films grown by the PAD technique, a CSD method for preparing oxide thin films.[17-19] Our finding indicates that the formation of V^{5+} and V^{3+} in the films could be greatly suppressed simply by introducing moisture during the conversion process. Moisture, a modest gas, which has been used to compensate for the oxygen vacancies in preparing other oxides,[20, 21] should be able to suppress the formation of V^{3+} ions. On the other way, moisture is not active enough to oxidize V^{4+} ions into V^{5+} ions. [22, 23] Moreover, it is easy to introduce moisture into the annealing environment of a CSD process. With this approach, we developed a unique technique to broaden the optimal growth window for VO_2 films, which can significantly enhance the film quality and the reproducibility. A very sharp MIT with a large resistivity change of 4 orders in magnitude has been reproducibly achieved. Especially, this scalable technique for fabricating wafer-scaled (3 inches in diameter) VO_2 films with uniform MIT properties has been demonstrated, which can pave a novel way for practical device developments.

To achieve stoichiometric VO_2 thin films, one should pay close attention to the interplay between the oxygen partial pressure pO_2 and the temperature during the conversion process. As shown in Figure 1 (a) (the blue line), the VO_2 film would be thermodynamically over-oxidized (pO_2, T_1) or over-reduced (pO_2, T_2) at a given oxygen pressure if the temperature was either lower or higher than the optimal temperature (pO_2, T). In other words, the film would show either oxygen rich (equivalent to vanadium vacancies) or oxygen deficient (equivalent to oxygen vacancies) when the temperature was below or above the optimal temperature. When the moisture is introduced during the conversion process, compensation for the oxygen vacancies could be achieved, [20, 21] resulting in the expansion of the growth window to a higher temperature range which is a relatively over-reduced environment. The reaction between oxygen vacancies and H_2O can be described by the following reaction:

$$V_O^{\bullet\bullet} + H_2O + 2e^{'} \leftrightarrow O_O + H_2$$ ……………………………………………………………(1)
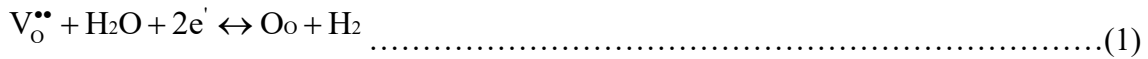
Moreover, introducing water vapor brings out another factor in the phase diagram, i.e. changing the chemical equilibrium. To evaluate the oxidability of water with the temperature and the equilibrium oxygen pressure, we need to consider the chemical equilibrium of the formation reaction of water:

$$\frac{1}{2}O_2 + H_2 \leftrightarrow H_2O$$ ……………………………………………………..…(2)
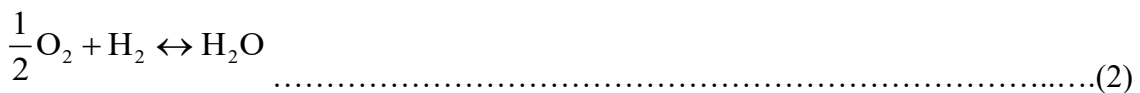
According to the chemical equilibrium constants of this formation reaction at different temperatures,[12] we can calculate one gas partial pressure when we know the other two kinds of gas partial pressures. For example, in our experiments, we used a formming gas (98.5% N_2 and 1.5% H_2) in the annealing process which set up the hydrogen partial pressure to be 0.015 atm. On the other hand, the equilibrium oxygen partial pressure pO_2 in Figure 1(a) for the formation of VO_2 at

500°C is about $10^{-39.2}$ atm. Then we can get the optimal water partial pressure is $3.2×10^{-8}$ atm at 500°C. If the water partial pressure was fixed to $3.2×10^{-8}$ atm. The equilibrium oxygen partial pressure pO_2 with temperature would be calculated and shown by the yellow line in Fig. 1(b). To have a better understanding of the important role of water, the equilibrium oxygen partial pressure pO_2 for the formation of VO_2 is also presented in Figure 1(b). It is obvious that the equilibrium oxygen partial pressure pO_2 for water can increase with temperature, which approaches the equilibrium oxygen partial pressure pO_2 for VO_2. In other words, introducing moisture in the growth ambience would set up a self-adjusted process for oxygen partial pressure while the growth temperature varies, which broadens the growth window of stoichiometric VO_2 thin films. If the water partial pressure was lower than $3.2×10^{-8}$ atm, e.g. $3.2×10^{-9}$ atm, the equilibrium oxygen partial pressure (presented in the green line in Figure 1(b)) would move downward, indicating that with a higher percentage of moisture, the optimal growth temperature window would shift to higher temperatures.
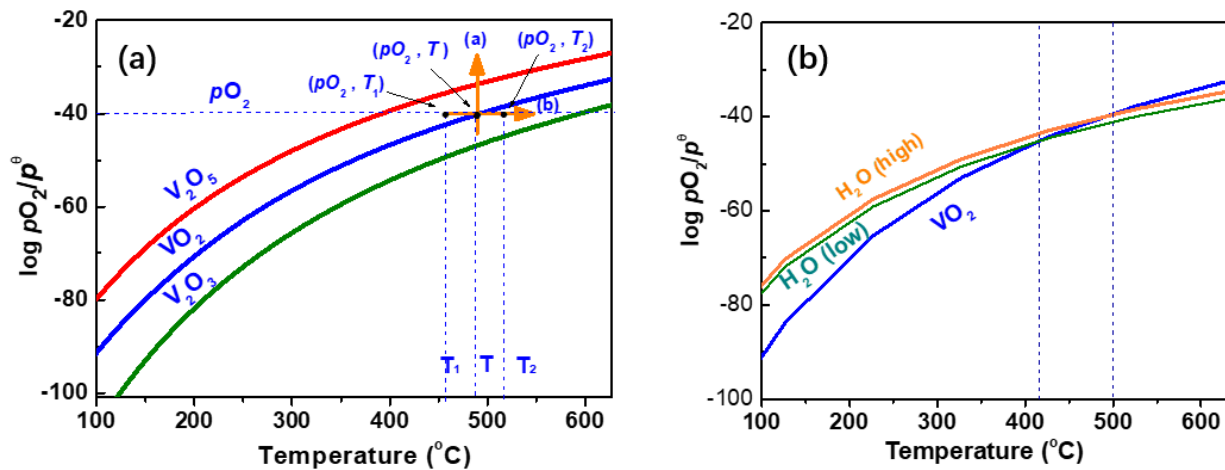

Figure 1 (a) Equilibrium oxygen partial pressure pO_2 *vs*. *T* curves for V_2O_3, VO_2 and V_2O_5, respectively. p^θ is standard atmospheric pressure. (b) Equilibrium oxygen partial pressure pO_2 *vs*.

T curves for VO_2 and H_2O, respectively. The equilibrium oxygen partial pressure for H_2O is calculated by setting the partial pressure of H_2 at 0.015 atm and the partial pressure of H_2O at 3.2×10^{-8} atm (high) and 3.2×10^{-9} atm (low), respectively. (the equilibrium constant of the formation reaction of H_2O with temperature is from Ref. [10])

2. EXPERIMENTAL SECTION

To explore the proposed approach for controlling the oxygen stoichiometry by moisture, various groups of samples were prepared to study the effects of the moisture on the growth window and the properties of VO_2 thin films. First, a solution containing vanadium ions and polyethyleneimine (PEI) was prepared.[24, 25] Briefly, 2 g of PEI (from Alfa Aesar, average Mw $\approx$ 10000) and 2 g of Ethylenediaminetetraacetic acid (EDTA) (from Alfa Aesar) were dissolved in 40 mL of de-ionized water. Then, 1 g of ammonium metavanadate (NH_3VO_3) (from Alfa Aesar) was added into this as-prepared solution and stirred until it was totally dissolved. The NH_4^+ ions in the solution were removed by an Amicon filtration. The concentration of V ions in the final precursor was determined to be 0.268 mmol/mL, as measured by inductively coupled plasma-atomic emission spectrometer (ICP-AES). The as-prepared precursor solution was spin-coated on M-plane sapphire [Al_2O_3 (10 $\overline{1}$0)] substrates at 7000 rpm for 40 s to form the precursor films. The quality of M-plane sapphire substrates, purchased from MTI Corporation, was checked by X-ray diffraction, as shown in Figure S2. The films were then thermally treated in a tube furnace. The precursor films were heated to 450°C at the speed of 1°C/min and kept at this temperature for 2 hours for the purpose of removing the polymer. Then the films were heated to the annealing temperature and kept at that temperature for 2 hours to crystallize the films. Forming gas (98.5% N_2 and 1.5% H_2) was used during the heat treatment to provide a balanced environment with a proper equilibrium oxygen partial pressure. [26, 27] The moisture was added to the forming gas by

using a home-made equipment as shown in Figure S3 in supporting information. Although the calculated optimal moisture partial pressure is 3.2×10^{-8} atm as shown in Figure 1 (b), it should be noted that the chemical reaction rate for water thermal decompostion at a low temperature is extremely low. In our experiment, the chemical equilibrium could not be reached. On the other hand, the oxygen partial pressure in preparing VO_2 films was much higher than the calculated equilibrium partial pressure shown in Figure 1 (a) from other experiments[4, 13, 14], due to the difference between the oxygen partial pressure in the growing VO_2 thin film material and that in the tube furnace. Considering these reasons, the real moisture partial pressure in the growth chamber should be much greater than the calculated value to validate the self-adjusted compensation effect. Thus, in our experiments, group I was prepared in an ambiance with no moisture as a reference sample group, while group II and group III were grown in the ambiance with 3.1% and 5.5% moisture, respectively. For each moisture concentration, the growth window was carefully evaluated by growing samples at various annealing temperatures in a certain range near the optimal growth tempareature.

3. RESULTS AND DISCUSSION

The as-prepared VO_2 films grown with or without moisture near the optimal growth tempareature are all epitaxy as confirmed by the normal *θ-2θ* scans and *ϕ*-scan using a PANalytical-Empyrean diffractometer, as shown in Figure 2 (a).The rocking curve measurements confirm that the crystallinity of the films can be improved with a moisture environment during the conversion process. As shown in Figures 2 (b) and (c), the values of the full width at half maximum (FWHM) of the rocking curves for the optimized VO_2 films grown with 5.5% and without moisture are 0.32º and 0.40º, respectively. The smaller value for the VO_2 films grown with moisture should be attributed to better crystal quality. The surface morphology of the films grown at different

moisture were examined by scanning electron microscopy (SEM), as shown in Figure S4. It presents that the moisture has little influence on the surface morphology of the films.
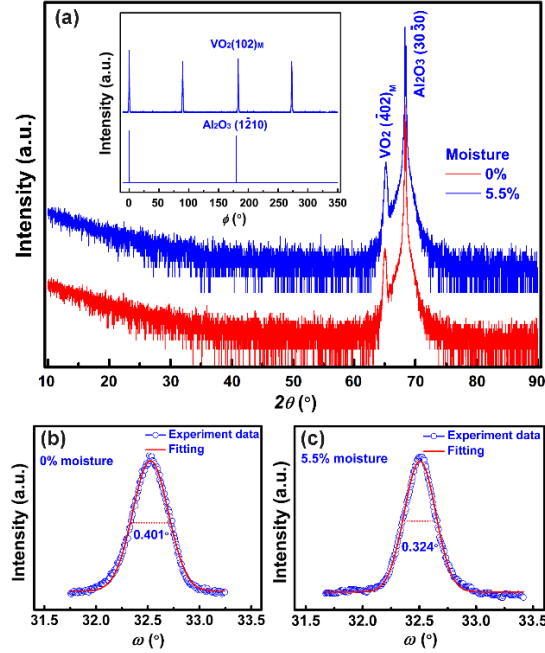

Figure 2 (a) The XRD θ-2θ scanning patterns of the VO$_2$ films, where the inset shows the XRD ϕ-scan patterns of the VO$_2$ film and the substrate; (b) and (c) the XRD rocking curves of the VO$_2$ films converted with and without moisture.

Resistivity (ρ) versus temperature (T) was measured for all the as-prepared samples. The ρ-T curves for the samples are shown in Figure S5-7 in the supporting information. Figures 3 (a) is the plot of $\Delta\rho/\rho_{80°C}$ *vs.* growth temperature for the three groups of samples, where $\Delta\rho=\rho_{50°C} - \rho_{80°C}$, $\rho_{50°C}$ and $\rho_{80°C}$ represent the resistivity of the VO$_2$ film at 50°C and 80°C, respectively. The growth window was defined to be the range of the growth temperature for the VO$_2$ thin films with $\Delta\rho/\rho_{80°C} > 2\times10^3$, as indicated in the inset of Figure 3 (b). As shown in Figure 3 (a), the growth window for the VO$_2$ thin films from group I (no moisture) is only about 4°C. However, the growth window for group II with 3.1% moisture expands to 12°C. Results from group III shows that when

the moisture concentration in the growth ambiance is further increased to 5.5%, the growth window can be as much as 36°C. Figure 3 (b) summarizes the growth window versus the moisture concentration. Obviously, the introduction of moisture can greatly broaden the growth window of the VO$_2$ films with desired properties, i.e. from 4°C for the case with 0% moisture to 36°C for that with 5.5% moisture. From Figure 3 (a), it can also be seen that the optimal growth window slightly shifts to a higher temperature when the concentration of moisture increases, which is consistent with the theoretical expectation illustrated in Figure 1 (b). Increasing the moisture means a higher equilibrium oxygen partial pressure. As shown in Figure 1(a), the temperature zone for the formation of VO$_2$ need to be increased with the increasing oxygen partial pressure to follow the equilibrium curve and avoid the formation of VO$_{2+x}$.
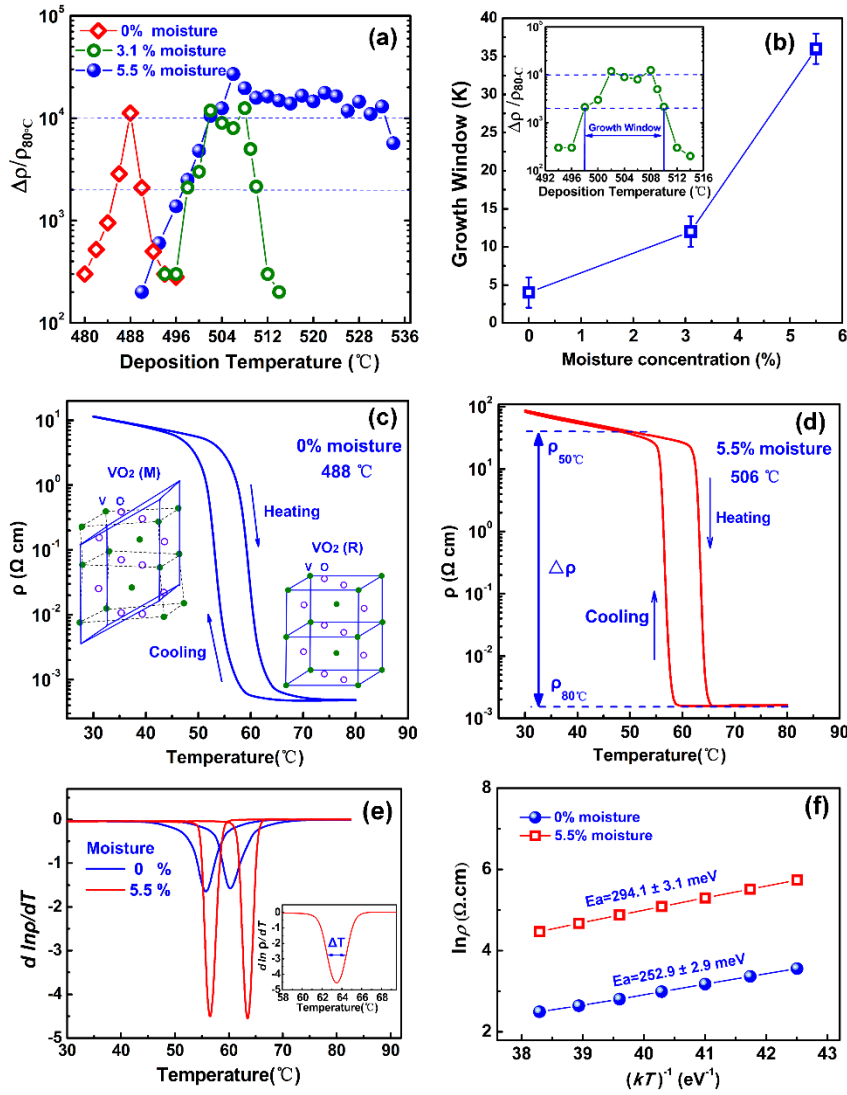
Figure 3 (a)The $\Delta\rho/\rho_{80°C}$ *vs. growth temperature* of the VO$_2$ thin films grown with 0%, 3.1% and 5.5% moisture; (b) growth windows for VO$_2$ thin films grown under various moisture concentrations, the inset shows the definition of the growth window; (c) the ρ vs. T characteristic of the VO$_2$ film grown without moisture; (d) the ρ vs. T characteristic of the VO$_2$ film grown with 5.5% moisture; (e) dlnρ/dT *vs. T* of the samples grown at 0% and 5.5% moisture, the inset shows the definition of ΔT of the transition; (f) the lnρ-$1/kT$ plots of the optimized samples grown at 0% and 5.5% moisture, respectively.

The most important benefits from the moisture process are not only to drastically broaden the growth window thus effectively enhance the reproducibility, but also to significantly improve electrical properties of the as-grown VO$_2$ thin films. As seen in Figures 3 (c) and (d), the resistivity drop $\Delta\rho/\rho_{80°C}$ ($\Delta\rho = \rho_{50°C} - \rho_{80°C}$) is about 1.1×10^4 across the MIT for the optimal VO$_2$ film grown without moisture but becomes about 2.75×10^4 for the optimal VO$_2$ film grown with 5.5% moisture. It is important to note that the transition width ΔT (defined as the full width at half maximum of the $\mathrm{d}\ln\rho/\mathrm{d}T$-$T$ plot [15, 28]) gets considerably improvement, or change from 3.5°C for the film grown without moisture to less than 1°C for the film grown with 5.5% moisture, as seen in Figure 3 (e). The sharp transition width of <1°C is comparable to that from the bulk single crystal,[29] suggesting that the films grown under the 5.5% moisture has good crystallinity. It is known that ΔT strongly depends on the presence of defects and strains in the films. Usually, the ΔT is proportional to the total defects in the films, or can be expressed as [30]

$$\Delta T \propto C_t \times \rho_d \quad\text{...(3)}$$

where C_t is a constant, ρ_d is the overall defect density. The narrow transition width of the film grown with 5.5% moisture implies the significant reduction of the defect density in the films or the high stoichiometric quality.

The improved film quality can also be understood by considering the point defects associated with non-stoichiometry such as the existence of V^{3+} ions (with a 3d^2 configuration). Here, VO$_2$ behaves as a n-type semiconductor. Based on the Boltzmann distribution function under the thermal equilibrium condition, the electron density can be expressed as:

$$P(N) = 2[\frac{2\pi m_n kT}{h^2}]^{\frac{3}{2}} \exp(-\frac{\Delta E_a}{kT}) \quad\text{...(4)}$$

where k is the Boltzmann constant, m_n is the effective mass of electron, h is the Planck constant, ΔE_a is the activation energy which is defined as the gap between the Fermi level E_F and the bottom of the conduction band E_c, i.e., $\Delta E_a = E_c - E_F$. The Fermi level E_F will shift closer to E_c (i.e., a smaller ΔE_a) for a relatively higher electron concentration. For epitaxial VO_2 films, the resistivity exhibits Arrhenius dependence which can be expressed as: [11]

$$\ln \rho = \ln \rho_0 + \frac{\Delta E_a}{kT} \qquad\qquad\qquad\qquad\qquad\qquad\qquad\qquad\qquad (5)$$

where ρ_0 is the resistivity at infinite high temperature. The $\ln\rho$-$1/kT$ plots were shown in Figure 3 (f). The values of ΔE_a can be determined by fitting the plots, which are 252.9 ± 2.9 meV and 294.1 ± 3.1 meV for the films grown without moisture and with 5.5% moisture, respectively. The band gap of VO_2 is about 0.6 eV. For ideal VO_2, the Fermi level E_F is located at the center of the band gap, so the activation energy ΔE_a for ideal VO_2 is about 300 meV. The fewer defects and the higher oxygen stoichiometry of the VO_2 film, the closer to 300 meV the activation energy will be. The activation energy data of our samples, 252 and 294 meV, indicate good crystalline quality of both films. On the other hand, the activation energy of the optimal film grown with 5.5% moisture increased 42 meV compared with that of the film grown without moisture. The change value is comparable to the modulation induced by strain reported by other researchers.[11] In other words, the film grown without moisture has a smaller value of ΔE_a than the one grown with 5.5% moisture, suggesting the former one possesses a higher charge carrier density which results in a lower resistivity. On the other hand, the local point defects associated with V^{3+} ions in VO_2 could interrupt the V-V dimers nearby and induce local stress. Both factors would degenerate or clamp the phase transition of VO_2. The higher electron density can also reduce the Thomas-Fermi screening length L_{TF}, which will effectively reduce the electron correlation and lead to a lower transition temperature. This could also explain our experimental observation where the MIT occurs

at 60.3°C for films grown without moisture, but at 64.5°C for the films grown with 5.5% moisture. The lower electron density in the film grown with moisture could be attributed to the aforementioned self-adjusted process for oxygen partial pressure by moisture, especially when the temperature in the tube furnace slightly varied to a higher value which may be over-reduced and inducing more V^{3+} ions in the film.

A Renishaw Micro-Raman Spectroscopy System with a 532 nm Raman exciting laser was used to confirm the phase quality of the VO_2 film grown in moisture environment. It is known that the low temperature M-phase of VO_2 is a polymorph that may contain two very similar phases: M1- and M2-phase.[7, 25] In general, VO_2 films grown on Al_2O_3 substrates are dominated by M1-phase. The M2-phase may occur and co-exist with the M1-phase when the films contain defects or stress.[25] Figures 4 (a) and (b) show the Raman spectra collected at different temperatures for our VO_2 films grown without moisture and with 5.5% moisture, respectively. As can be seen from the spectra, the intensity of 610 cm^{-1} Raman peak (the M1 phase) became weaker with increasing temperature for VO_2 films grown either with or without moisture. However, a small amount of 646 cm^{-1} Raman peak, the fingerprint for M2-phase, was detected for the sample grown without moisture as shown in Figure 4 (c) from the Lorentz fitting. Yet no detectable M2-phase was found in the film grown with 5.5% moisture (Figure 4 (d)). The formation of M2-phase in the films grown without moisture is highly possibly related to the point defects in the films. Therefore, the absence of M2-phase in the films grown with 5.5% moisture clearly suggests less defect density in the film, or the high crystallinity of the film. As already indicated in literatures,[25, 31] the absence of M2 phase would also be a contributor to the better MIT performance of the films grown with appropriate concentration of moisture.
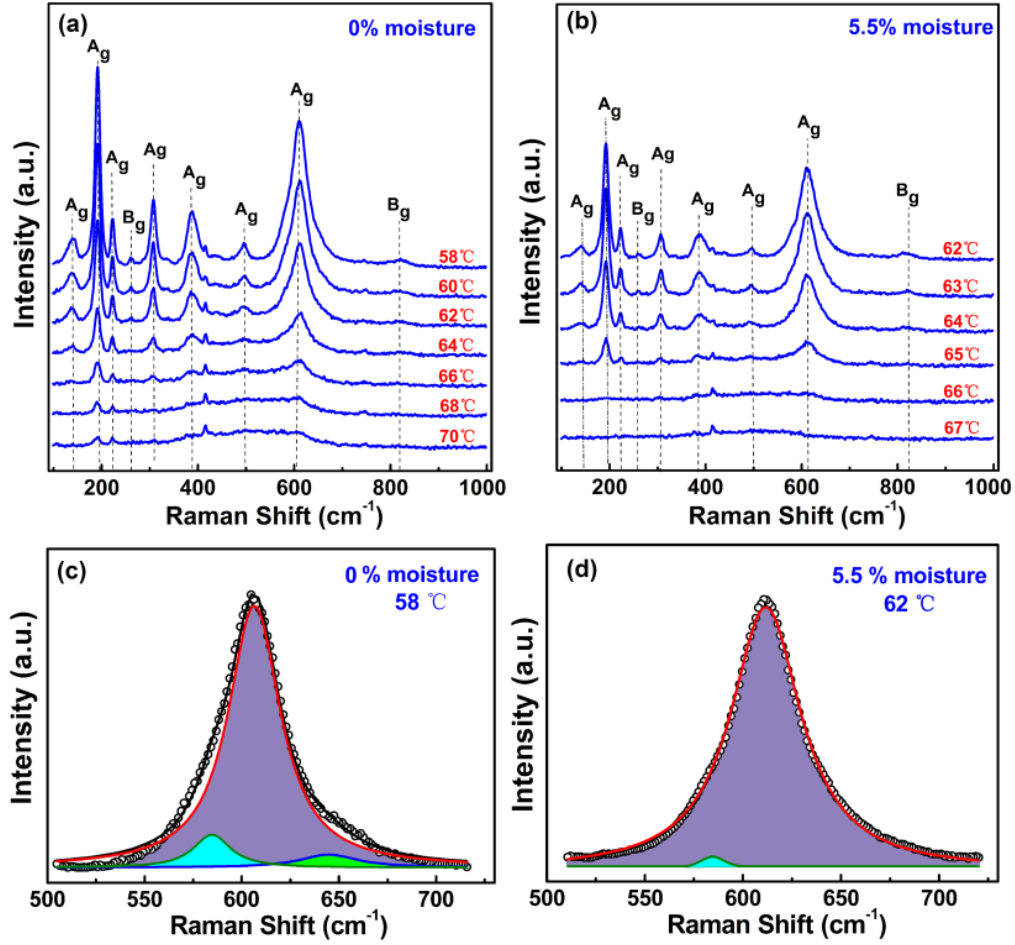
Figure 4 The Raman spectra measured at various temperatures for the VO₂ films grown without moisture (a) and with 5.5% moisture (b), respectively; Lorentz fitting results of the Raman spectra for the samples grown without moisture (c) and with 5.5% moisture (d), measured at 58°C and 62°C , respectively. (*The fitting peak near 585 cm^{-1} is the E_g mode of the sapphire substrate.).

It has been reported that when the oxidation is performed in a dry atmosphere, the transport of oxygen in the oxide depends on the decomposition of the oxide, and the oxygen partial pressure pO_2 inside the oxide is lower than that near the surface.[32] Accordingly, even when the VO₂ thin film is grown in an optimal ambiance, the oxygen partial pressure near the Al₂O₃/VO₂ interface

would be relatively lower than that near the surface. In other words, no matter how carefully we optimize the growth ambiance, we cannot make both the surface and interface of VO_2 thin films under an optimal growth condition. Since the valence state of VO_2 is extremely sensitive to pO_2, the thin films are always stoichiometrically inhomogeneous through the film thickness. It was also reported that an oxidize-reduce system of H_2O-H_2 will be built up in the oxide when moisture exists in the growth atmosphere, which will enhance the transport of O_2 in the oxide, and hence reduce the deviation of oxygen partial pressure between the surface and the interface. [32] Thus, if moisture is presented in the growth ambiance, the oxygen partial pressure near the surface and near the Al_2O_3/ VO_2 interface will be closer to each other than the case without moisture, which will greatly improve the stoichiometric homogeneity of VO_2 thin films. The improvement of the homogeneity would certainly enhance the MIT performance of the thin films, especially reduce the transition width of MIT.

In order to investigate the stoichiometric homogeneity of the VO_2 films more accurately, X-ray photoelectron spectroscopy (XPS) depth profile were collected and compared for the optimized VO_2 films grown with 0% and 5.5% moisture, as shown in Figure 5. To minimize the damages of the component in the VO_2 film, a Thermo scientific ESCALAB 250 XI spectrometer was employed. The values of x (VO_x, x=O:V, for stoichiometric VO_2, x=2) for both samples at their surfaces are about 2.3. This is because that the surfaces of both samples were oxidized in the air. When the depth is 10 nm, the values of x are close to 2 for both samples. The values of x become smaller at deeper positions. However, it is very clearly shown that the value of x reduces slower for the optimal sample grown with 5.5% moisture than the one grown with 0% moisture. When the depth position changes from 10 nm to 40 nm (where is the VO_2/Al_2O_3 interface), the former one dropped 0.085 while the latter one dropped 0.139. In other words, the optimal sample grown

with 5.5% moisture is with better stoichiometric homogeneity through the thickness of the film. This result indicate that the moisture in the growth ambiance does improve the oxygen transport and make the VO$_2$ films more stoichiometric homogenous.
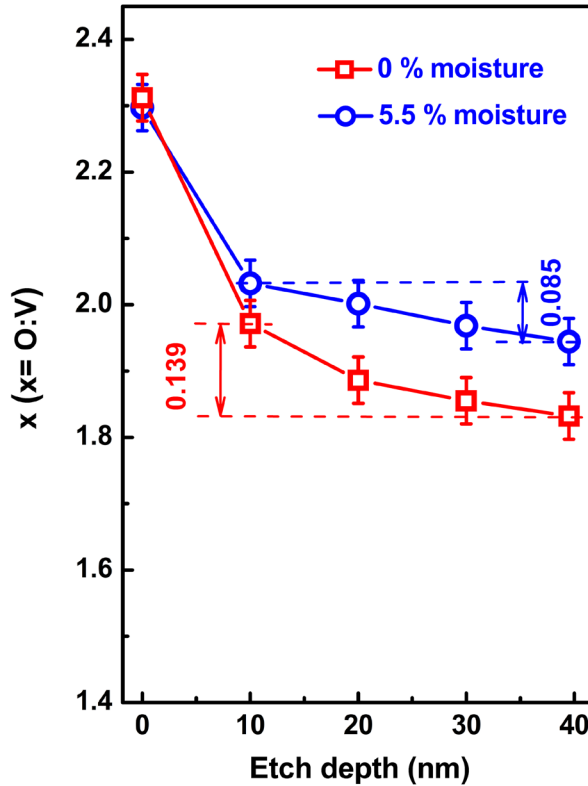

Figure 5 XPS depth profile of the optimal VO$_2$ films grown with 0% and 5.5% moisture, respectively.

Transmission electron microscopy (TEM) and electron energy loss spectroscopy (EELS) were also employed to examine the microstructure of the optimized VO$_2$ film with a nominal film thickness around 38 nm grown with 5.5% moisture. Figures 6 (a) and (b) show the cross-sectional TEM image and selected area electron diffraction (SAED) pattern of the sample, respectively. The results indicate that the VO$_2$ film is epitaxially grown on the M-plane Al$_2$O$_3$ substrate with monoclinic structure (M1 phase with lattice parameters of a_{M1} = 5.752 Å, b_{M1}= 4.526 Å, c_{M1}=

5.382 Å, and β_{M1}= 122.6°).[24] Considering the monoclinic nature of VO$_2$, the epitaxial relationship was confirmed to be ($\bar{4}$02)VO$_2$||(10 $\bar{1}$0)Al$_2$O$_3$, [10 $\bar{2}$]VO$_2$|| [0001]Al$_2$O$_3$, as schematically shown in Figure 6 (c). The TEM results agree well with the XRD results. Figures 6 (d) and (e) are the cross-sectional high resolution TEM image and EELS data taken at different locations through the film thickness. The very similar low-energy loss spectra of VO$_2$ at different locations across the film thickness indicate that the film has good stoichiometric homogeneity.
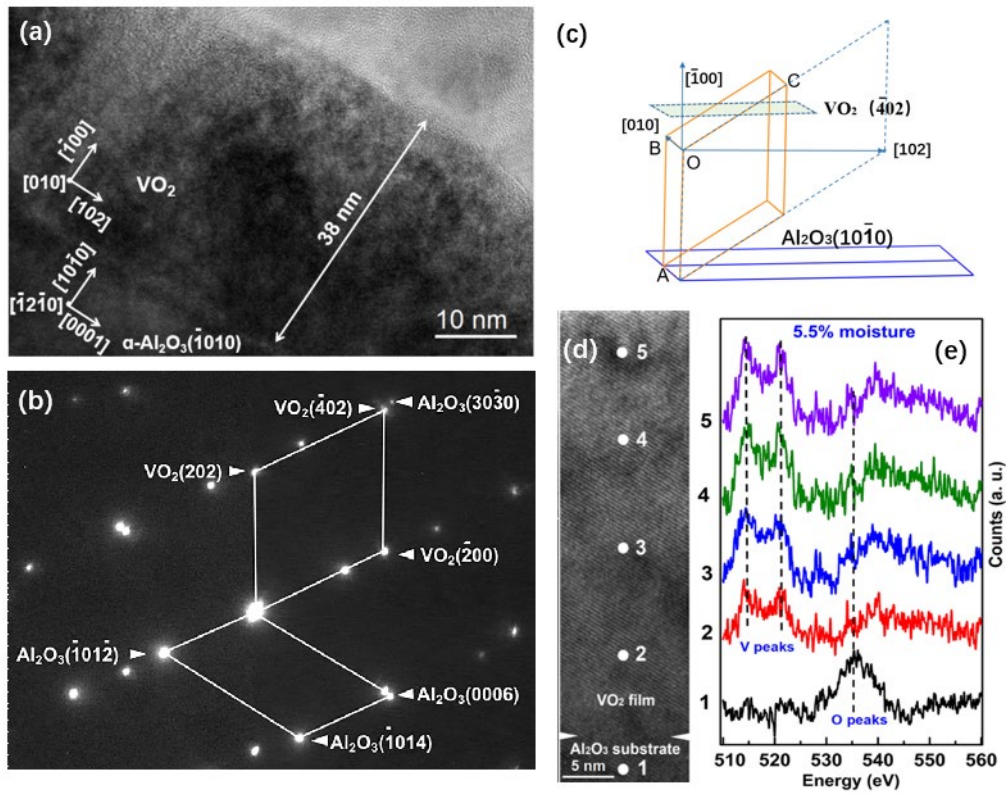

Figure 6 (a) and (b) show the cross-sectional TEM image and selected area electron diffraction (SAED) pattern of the optimized VO$_2$ film grown with 5.5% moisture. (c) Schematic of the epitaxial relationship between VO$_2$ and the substrate. The VO$_2$ ($\bar{4}$02) surface are indicated by a plane, which is almost parallel to the Al$_2$O$_3$ (10 $\bar{1}$0) surface. (d) and (e) are the cross-sectional

high resolution TEM image and EELS data taken at different locations through the film thickness of this sample.

To demonstrate the feasibility of this unique technique for fabricating scalable films on large scale substrates, a VO_2 thin film was synthesized on a 3-inch M-plane sapphire wafer in the ambiance with 3.1% moisture at 504°C. Figure 7 (a) is the picture of the 3-inch wafer coated with the VO_2 film. To check the uniformity of the VO_2 film on the 3-inch wafer, the electrical properties were characterized at different regions on the VO_2-coated-wafer. The contour map of $\Delta\rho/\rho_{80°C}$ of the VO_2 film on the wafer, as shown in Figure 7 (b), indicates that 100% of the tested regions on this wafer exhibit large resistivity drops of more than 7.5×10^3 across the MIT. The contour maps of ΔT (as seen in Figures 7 (c) and (d)) indicate that ΔT is about 3.2°C with a standard deviation of 0.6°C and T_c centered at 59.7°C with a standard deviation of 0.4°C . These results denote that the VO_2 film can be achieved on a 3-inch wafer with uniform properties by using this low-cost and scalable technique.
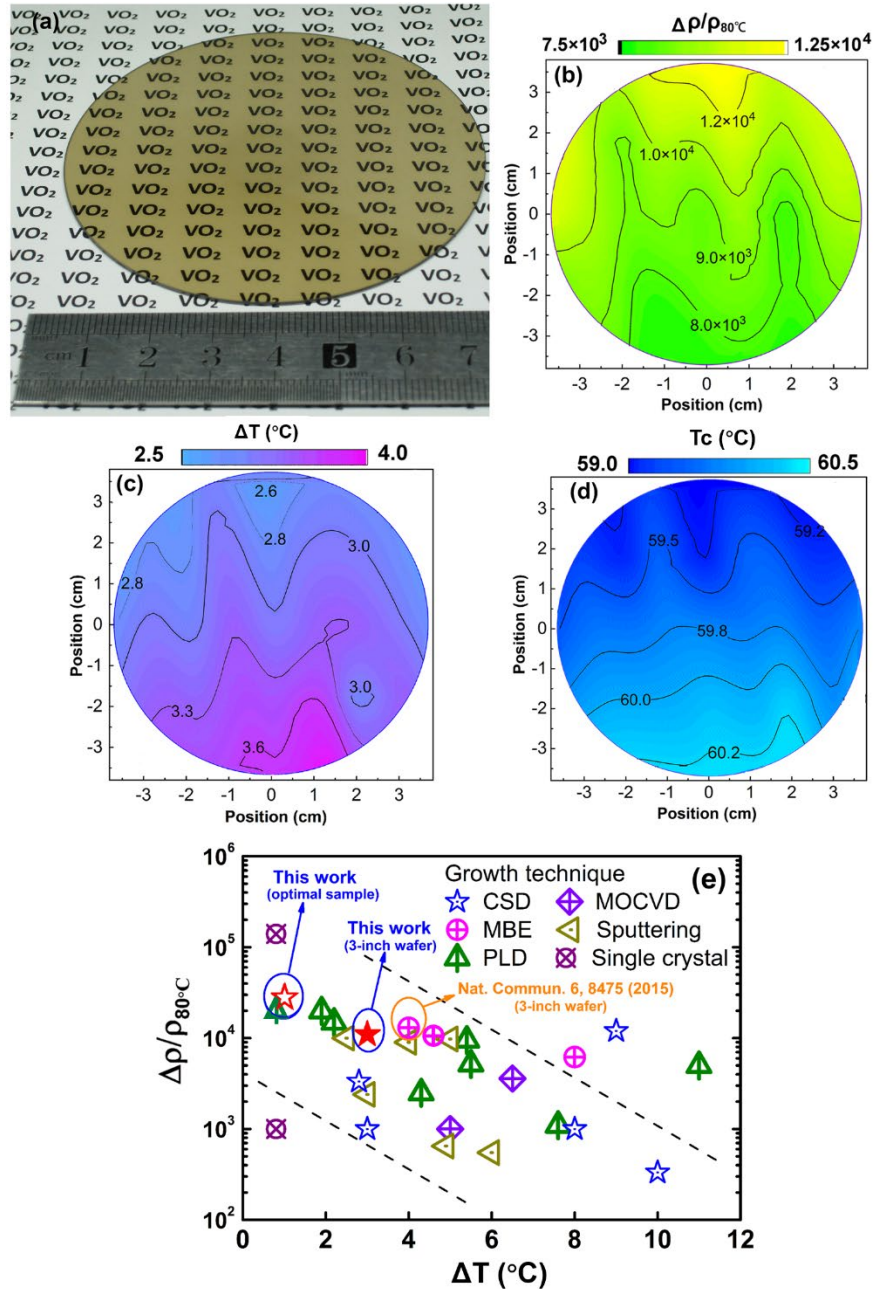
Figure 7 (a) The picture of the VO$_2$ thin film grown on a 3-inch M-plane sapphire wafer; (b)-(d) contour maps of $\Delta\rho/\rho_{80°C}$, ΔT and T_c of the VO$_2$ film on the wafer, respectively; (e) benchmark of resistivity-drop $\Delta\rho/\rho_{80°C}$ and ΔT for VO$_2$ samples grown by using various techniques from Refs.[131]-[15], [24], [29], [33]-[47]. The values of resistivity-drop $\Delta\rho/\rho_{80°C}$ from some literatures have been re-calculated basing on the same temperature range.

Figure 7 (e) is the summary of some recent research data collected from literatures for the fabrication of single crystal VO$_2$ samples[29, 33] and VO$_2$ thin films by using various techniques such as CSD, [24, 34, 35] MBE,[36-38] PLD,[13-15, 39, 40] metal organic chemical vapor deposition (MOCVD)[41, 42] and sputtering[43-47]. Our research clearly demonstrated that our moisture-assisted large dimensional and low cost PAD growth technique can significantly enhance the quality of epitaxial VO$_2$ thin films with physical properties comparable to the ones from high cost MBE and PLD techniques. These results indicate that the as-developed moisture-assisted PAD technique can effectively control the oxygen stoichiometry in VO$_2$ thin films and overcome the difficulty in the fabrication of high quality VO$_2$ thin films with large areas for practical device applications.

4. CONCLUSIONS

In summary, a moisture-assisted chemical solution deposition technique (polymer-assisted deposition) was developed for fabricating the scalable, uniform, highly epitaxial VO$_2$ films. The use of moisture during the conversion process can significantly enhance the quality of VO$_2$ thin films. By introducing a proper amount of moisture, VO$_2$ thin films with a resistivity drop of about 2.75×10^4 times, and a transition width ΔT of 1°C across the MIT were successfully achieved. Especially, a much broader growth window of 36°C with the assistance of moisture, expanded from the narrow growth window of 4°C with no moisture, enables ones to achieve reproducible high quality VO$_2$ films with uniform properties on scalable wafers. The results are attributed to the improvements in controlling the oxygen stoichiometry in the films, via the compensation of oxygen vacancies and a self-adjusted process for oxygen partial pressure at different temperatures by introducing moisture. These achievements would pave a novel way for large area, low cost, and high quality VO$_2$ film technology from the laboratory researches to practical industrial applications.

ASSOCIATED CONTENT

Supporting Information.

The following files are available free of charge.

The phase diagram of VO_x system, the schematic for the home-made equipment to produce moisture and the ρ-T curves of the VO_2 thin films grown at various temperatures and with different moisture concentrations. (PDF)

AUTHOR INFORMATION

Corresponding Author

*mingao@uestc.edu.cn.

* linyuan@uestc.edu.cn.

Author Contributions

The manuscript was written through contributions of all authors. All authors have given approval to the final version of the manuscript.

Notes

The authors declare no competing financial interest.

REFERENCES

(1)   Morin, F. J., Oxides which show a metal-to-insulator transition at the neel temperature. *Phys. Rev. Lett.* **1959,** *3*, 34-36.

(2)   Yang, Z.; Ko, C.; Ramanathan, S., Oxide Electronics Utilizing Ultrafast Metal-Insulator Transitions. *Annu. Rev. Mater. Res.* **2011,** *41*, 337-367.

(3)   Wu, C.; Feng, F.; Xie, Y., Design of vanadium oxide structures with controllable electrical properties for energy applications. *Chem. Soc. Rev.* **2013,** *42*, 5157-5183.

(4)   Jeong, J.; Aetukuri, N.; Graf, T.; Schladt, T. D.; Samant, M. G.; Parkin, S. S. P., Suppression of Metal-Insulator Transition in VO_2 by Electric Field–Induced Oxygen Vacancy Formation. *Science* **2013,** *339*, 1402-1405.

(5)   Park, J. H.; Coy, J. M.; Kasirga, T. S.; Huang, C.; Fei, Z.; Hunter, S.; Cobden, D. H., Measurement of a solid-state triple point at the metal-insulator transition in VO_2. *Nature* **2013,** *500*, 431-434.

(6)   Lee, J.; Lee, D.; Cho, S. J.; Seo, J.-H.; Liu, D.; Eom, C.-B.; Ma, Z., Epitaxial VO2 thin film-based radio-frequency switches with thermal activation. *Appl. Phys. Lett.* **2017,** *111*, 063110.

(7)   Katzke, H.; Tolédano, P.; Depmeier, W., Theory of morphotropic transformations in vanadium oxides. *Phys. Rev. B* **2003,** *68*, 024109.

(8)   Zhang, S.; Kim, I. S.; Lauhon, L. J., Stoichiometry Engineering of Monoclinic to Rutile Phase Transition in Suspended Single Crystalline Vanadium Dioxide Nanobeams. *Nano Lett.* **2011,** *11*, 1443-1447.

(9)   Hong, W.-K.; Park, J. B.; Yoon, J.; Kim, B.-J.; Sohn, J. I.; Lee, Y. B.; Bae, T.-S.; Chang, S.-J.; Huh, Y. S.; Son, B.; Stach, E. A.; Lee, T.; Welland, M. E., Hydrogen-Induced Morphotropic Phase Transformation of Single-Crystalline Vanadium Dioxide Nanobeams. *Nano Lett.* **2013,** *13*, 1822-1828.

(10)   Fan, L. L.; Chen, S.; Wu, Y. F.; Chen, F. H.; Chu, W. S.; Chen, X.; Zou, C. W.; Wu, Z. Y., Growth and phase transition characteristics of pure M-phase VO_2 epitaxial film prepared by oxide molecular beam epitaxy. *Appl. Phys. Lett.* **2013,** *103*, 131914.

(11)   Chen, C.; Zhao, Y.; Pan, X.; Kuryatkov, V.; Bernussi, A.; Holtz, M.; Fan, Z., Influence of defects on structural and electrical properties of VO_2 thin films. *J. Appl. Phys.* **2011,** *110*, 023707.

(12)   Barin, I., In *Thermochemical Data of Pure Substances*, Wiley-VCH Verlag GmbH: 2008.

(13)   Lee, S.; Meyer, T. L.; Park, S.; Egami, T.; Lee, H. N., Growth control of the oxidation state in vanadium oxide thin films. *Appl. Phys. Lett.* **2014,** *105*, 223515.

(14)   Kim, H.; Charipar, N.; Osofsky, M.; Qadri, S. B.; Piqué, A., Optimization of the semiconductor-metal transition in VO_2 epitaxial thin films as a function of oxygen growth pressure. *Appl. Phys. Lett.* **2014,** *104*, 081913.

(15)   Lee, D.; Lee, J.; Song, K.; Xue, F.; Choi, S.-Y.; Ma, Y.; Podkaminer, J.; Liu, D.; Liu, S.-C.; Chung, B.; Fan, W.; Cho, S. J.; Zhou, W.; Lee, J.; Chen, L.-Q.; Oh, S. H.; Ma, Z.; Eom, C.-B., Sharpened VO2 Phase Transition via Controlled Release of Epitaxial Strain. *Nano Lett.* **2017,** *17*, 5614-5619.

(16) Martens, K.; Aetukuri, N.; Jeong, J.; Samant, M. G.; Parkin, S. S. P., Improved metal-insulator-transition characteristics of ultrathin VO_2 epitaxial films by optimized surface preparation of rutile TiO_2 substrates. *Appl. Phys. Lett.* **2014,** *104*, 081918.

(17) Jia, Q. X.; McCleskey, T. M.; Burrell, A. K.; Lin, Y.; Collis, G. E.; Wang, H.; Li, A. D. Q.; Foltyn, S. R., Polymer-assisted deposition of metal-oxide films. *Nat. Mater.* **2004,** *3*, 529-532.

(18) Liang, W.; Ji, Y.; Nan, T.; Huang, J.; Bi, Z.; Zeng, H.; Du, H.; Chen, C.; Jia, Q.; Lin, Y., Growth Dynamics of Barium Titanate Thin Films on Polycrystalline Ni Foils Using Polymer-Assisted Deposition Technique. *ACS Appl. Mater. Interfaces* **2012,** *4*, 2199-2203.

(19) Luo, H.; Wang, H.; Bi, Z.; Feldmann, D. M.; Wang, Y.; Burrell, A. K.; McCleskey, T. M.; Bauer, E.; Hawley, M. E.; Jia, Q., Epitaxial Ternary Nitride Thin Films Prepared by a Chemical Solution Method. *J. Am. Chem. Soc.* **2008,** *130*, 15224-15225.

(20) Zhang, H.; Yang, J.; Liu, H.; Wang, S., Meter-long $CeO_2/YSZ/Y_2O_3$ buffer layers for YBCO coated conductors using DC reactive sputtering. *Physica C: Superconductivity* **2010,** *470*, 1998-2001.

(21) Yuanqing, C.; Xinni, T.; Weibai, B.; Mengjuan, L.; Ping, J.; Gaoyang, Z., All chemical solution deposition of textured $YBa_2Cu_3O_{7-x}/Y_{0.2}Ce_{0.8}O_2/La_2Zr_2O_7$ multilayer films on biaxially textured NiW tape. *Supercond. Sci. Technol.* **2015,** *28*, 075015.

(22) Liu, J.; Li, Q.; Wang, T.; Yu, D.; Li, Y., Metastable Vanadium Dioxide Nanobelts: Hydrothermal Synthesis, Electrical Transport, and Magnetic Properties. *Angew. Chem.* **2004,** *116*, 5158-5162.

(23) Son, J.-H.; Wei, J.; Cobden, D.; Cao, G.; Xia, Y., Hydrothermal Synthesis of Monoclinic VO_2 Micro- and Nanocrystals in One Step and Their Use in Fabricating Inverse Opals. *Chem. Mater.* **2010,** *22*, 3043-3050.

(24)   Ji, Y. D.; Pan, T. S.; Bi, Z.; Liang, W. Z.; Zhang, Y.; Zeng, H. Z.; Wen, Q. Y.; Zhang, H. W.; Chen, C. L.; Jia, Q. X.; Lin, Y., Epitaxial growth and metal-insulator transition of vanadium oxide thin films with controllable phases. *Appl. Phys. Lett.* **2012,** *101*, 071902.

(25)   Ji, Y.; Zhang, Y.; Gao, M.; Yuan, Z.; Xia, Y.; Jin, C.; Tao, B.; Chen, C.; Jia, Q.; Lin, Y., Role of microstructures on the M1-M2 phase transition in epitaxial VO_2 thin films. *Sci. Rep.* **2014,** *4*, 4854.

(26)   Dawley, J. T.; Clem, P. G., Dielectric properties of random and ⟨100⟩ oriented $SrTiO_3$ and $(Ba,Sr)TiO_3$ thin films fabricated on ⟨100⟩ nickel tapes. *Appl. Phys. Lett.* **2002,** *81*, 3028-3030.

(27)   Bretos, I.; Schneller, T.; Waser, R.; Hennings, D. F.; Halder, S.; Thomas, F., Compositional Substitutions and Aliovalent Doping of $BaTiO_3$-Based Thin Films on Nickel Foils Prepared by Chemical Solution Deposition. *J. Am. Ceram. Soc.* **2010,** *93*, 506-515.

(28)   Jian, J.; Chen, A.; Zhang, W.; Wang, H., Sharp semiconductor-to-metal transition of VO2 thin films on glass substrates. *J. Appl. Phys.* **2013,** *114*, 244301.

(29)   Yoshichika, B.; Koichi, N.; Yasutoshi, K.; Toshio, T., Growth of VO_2 Single Crystals by Chemical Transport Reaction. *Jpn. J. Appl. Phys.* **1969,** *8*, 633.

(30)   Narayan, J.; Bhosle, V. M., Phase transition and critical issues in structure-property correlations of vanadium oxide. *J. Appl. Phys.* **2006,** *100*, 103524.

(31)   Tselev, A.; Luk'yanchuk, I. A.; Ivanov, I. N.; Budai, J. D.; Tischler, J. Z.; Strelcov, E.; Kolmakov, A.; Kalinin, S. V., Symmetry Relationship and Strain-Induced Transitions between Insulating M1 and M2 and Metallic R phases of Vanadium Dioxide. *Nano Lett.* **2010,** *10*, 4409-4416.

(32)   Birks, N.; Meier, G. H., In *Introduction to high-temperature oxidation of metals*, Edward Arnold: London, 1983.

(33)   Sasaki, H.; Watanabe, A., A New Growing Method for VO_2 Single Crystals. *J. Phys. Soc. Jpn.* **1964,** *19*, 1748-1748.

(34)   Shi, Q.; Huang, W.; Zhang, Y.; Yan, J.; Zhang, Y.; Mao, M.; Zhang, Y.; Tu, M., Giant Phase Transition Properties at Terahertz Range in VO_2 films Deposited by Sol–Gel Method. *ACS Appl. Mater. Interfaces* **2011,** *3*, 3523-3527.

(35)   Guo, Y.; Xu, H.; Zou, C.; Yang, Z.; Tong, B.; Yu, J.; Zhang, Y.; Zhao, L.; Wang, Y., Evolution of structure and electrical properties with annealing time in solution-based VO_2 thin films. *J. Alloys Compd.* **2015,** *622*, 913-917.

(36)   Zhang, H.-T.; Zhang, L.; Mukherjee, D.; Zheng, Y.-X.; Haislmaier, R. C.; Alem, N.; Engel-Herbert, R., Wafer-scale growth of VO_2 thin films using a combinatorial approach. *Nat. Commun.* **2015,** *6*, 8475.

(37)   Tashman, J. W.; Lee, J. H.; Paik, H.; Moyer, J. A.; Misra, R.; Mundy, J. A.; Spila, T.; Merz, T. A.; Schubert, J.; Muller, D. A.; Schiffer, P.; Schlom, D. G., Epitaxial growth of VO_2 by periodic annealing. *Appl. Phys. Lett.* **2014,** *104*, 063104.

(38)   Thery, V.; Boulle, A.; Crunteanu, A.; Orlianges, J. C.; Beaumont, A.; Mayet, R.; Mennai, A.; Cosset, F.; Bessaudou, A.; Fabert, M., Structural and electrical properties of large area epitaxial VO2 films grown by electron beam evaporation. *J. Appl. Phys.* **2017,** *121*, 055303.

(39)   Gupta, A.; Narayan, J.; Dutta, T., Near bulk semiconductor to metal transition in epitaxial VO_2 thin films. *Appl. Phys. Lett.* **2010,** *97*, 151912.

(40)   Yang, T.-H.; Aggarwal, R.; Gupta, A.; Zhou, H.; Narayan, R. J.; Narayan, J., Semiconductor-metal transition characteristics of VO_2 thin films grown on c- and r-sapphire substrates. *J. Appl. Phys.* **2010,** *107*, 053514.

(41)   Maruyama, T.; Ikuta, Y., Vanadium dioxide thin films prepared by chemical vapour deposition from vanadium(III) acetylacetonate. *J. Mater. Sci.* **1993,** *28*, 5073-5078.

(42)   Sahana, M. B.; Subbanna, G. N.; Shivashankar, S. A., Phase transformation and semiconductor-metal transition in thin films of VO_2 deposited by low-pressure metalorganic chemical vapor deposition. *J. Appl. Phys.* **2002,** *92*, 6495-6504.

(43)   Ba, C.; Bah, S. T.; D'Auteuil, M.; Ashrit, P. V.; Vallée, R., Fabrication of High-Quality VO_2 Thin Films by Ion-Assisted Dual ac Magnetron Sputtering. *ACS Appl. Mater. Interfaces* **2013,** *5*, 12520-12525.

(44)   Chen, C.; Zhu, Y.; Zhao, Y.; Lee, J. H.; Wang, H.; Bernussi, A.; Holtz, M.; Fan, Z., VO_2 multidomain heteroepitaxial growth and terahertz transmission modulation. *Appl. Phys. Lett.* **2010,** *97*, 211905.

(45)   Claassen, J. H.; Lu, J. W.; West, K. G.; Wolf, S. A., Relaxation dynamics of the metal-semiconductor transition in VO_2 thin films. *Appl. Phys. Lett.* **2010,** *96*, 132102.

(46)   Brassard, D.; Fourmaux, S.; Jean-Jacques, M.; Kieffer, J. C.; Khakani, M. A. E., Grain size effect on the semiconductor-metal phase transition characteristics of magnetron-sputtered VO_2 thin films. *Appl. Phys. Lett.* **2005,** *87*, 051910.

(47)   Zimmers, A.; Aigouy, L.; Mortier, M.; Sharoni, A.; Wang, S.; West, K. G.; Ramirez, J. G.; Schuller, I. K., Role of Thermal Heating on the Voltage Induced Insulator-Metal Transition in VO_2. *Phys. Rev. Lett.* **2013,** *110,* 056601.

Table of Contents

$$V_O^{\bullet\bullet} + H_2O + 2e' \rightarrow O_O + H_2$$